Regulation of voltage-gated calcium channel activity by the Rem and Rad GTPases

Brian S. Finlin*, Shawn M. Crump†, Jonathan Satin†, and Douglas A. Andres*‡

Departments of *Molecular and Cellular Biochemistry and †Physiology, University of Kentucky College of Medicine, Lexington, KY 40536-0298

Edited by William A. Catterall, University of Washington School of Medicine, Seattle, WA, and approved September 26, 2003 (received for review December 19, 2002)

Rem, Rem2, Rad, and Gem/Kir (RGK) represent a distinct GTPase family with largely unknown physiological functions. We report here that both Rem and Rad bind directly to Ca^{2+} channel β-subunits ($Ca_V\beta$) *in vivo*. No calcium currents are recorded from human embryonic kidney 293 cells coexpressing the L type Ca^{2+} channel subunits $Ca_V1.2$, $Ca_V\beta_{2a}$, and Rem or Rad, but $Ca_V1.2$ and $Ca_V\beta_{2a}$ transfected cells elicit Ca^{2+} channel currents in the absence of these small G proteins. Importantly, Ca_V3 (T type) Ca^{2+} channels, which do not require accessory subunits for ionic current expression, are not inhibited by expression of Rem. Rem is expressed in primary skeletal myoblasts and, when overexpressed in C2C12 myoblasts, wild-type Rem inhibits L type Ca^{2+} channel activity. Deletion analysis demonstrates a critical role for the Rem C terminus in both regulation of functional Ca^{2+} channel expression and β-subunit association. These results suggest that all members of the RGK GTPase family, via direct interaction with auxiliary β-subunits, serve as regulators of L type Ca^{2+} channel activity. Thus, the RGK GTPase family may provide a mechanism for achieving cross talk between Ras-related GTPases and electrical signaling pathways.

Rem, Rem2, Rad, and Gem/Kir (RGK) are members of a Ras-related GTPase subfamily (RGK family), with many unique characteristics that distinguish them from other members of the Ras superfamily (1–5). The common structure for all RGK proteins consists of a conserved Ras-related core domain, a series of nonconservative amino acid substitutions within regions known to be involved in guanine nucleotide binding and hydrolysis, a non-CAAX-containing C-terminal extension, and large N-terminal extensions relative to other Ras family proteins. The conservation of structural features within the RGK proteins suggests shared mechanisms of regulation and the control of common cellular signal transduction networks. However, RGK subfamily members differ from each other and from other Ras-related proteins in their putative effector (G2) domains, suggesting that they interact with distinct regulatory and effector proteins, and each exhibits distinct tissue-specific expression patterns (1–5). Thus, despite their conserved structural and biochemical properties, functional evidence to suggest a unified mechanism of action has been limited.

In this study, we investigated the ability of Rem and Rad to regulate Ca^{2+} channel activity. Our results demonstrate that, although both proteins have distinct effector interaction domains, they each bind directly to $Ca_V\beta$ subunits and inhibit detectable ionic current expression from the native cardiac L type, but not from T type, Ca^{2+} channels when coexpressed in human embryonic kidney (HEK)293 cells. The Rem protein is expressed in striated muscle cells, and we demonstrate that Rem inhibits L type Ca^{2+} channel activity in differentiated C2C12 myotubes. Deletion analysis demonstrates that the C terminus of Rem plays an important role in $Ca_V\beta$ subunit association and is necessary for regulation of channel activity. Taken together, these studies indicate that Rem functions as a potent regulator of L type Ca^{2+} channel function in muscle and suggest that a conserved physiological role for the RGK GTPase gene family is the control of Ca^{2+} channel activity via modulation of $Ca_V\beta$ subunit function.

Experimental Procedures

RNase Protection Assays and Cell Culture. C2C12DS and C2C12(E) mouse muscle myoblast cell lines were from Robert Krauss (Mount Sinai School of Medicine, New York) and were cultured and induced to differentiate as described (6). Primary mouse muscle cultures and MM14 cells were provided by Phillip Bonner (Department of Biology, University of Kentucky, Lexington). The culture of HEK293 cell lines was done as described (7). RNase protection assays were performed on 20 μg of total RNA from the indicated cell lines as described (1).

Immunoblotting Rem. A rabbit polyclonal antibody (5313) was generated against the Rem^{6-17} peptide (QQEAKTTLRRRA) (8) and affinity purified against the same peptide. The affinity-purified antibody was used at 1 μg/ml for all experiments. The horseradish peroxidase-conjugated goat anti-rabbit secondary antibody (Zymed) was used at a 1:20,000 dilution. Super Signal (Pierce) was used as the enhanced chemiluminescence reagent.

Electrophysiological Studies. HEK293 cells were transiently transfected with plasmids 12–48 h before recordings as described (9). Transfected cells were identified by the expression of GFP. The whole-cell configuration of the patch–clamp technique was used to measure Ca_V1 or Ca_V3 ionic current. Patch electrodes with resistances of 1–2 MΩ contained: 110 mM K-glucanate, 40 mM CsCl, 1 mM $MgCl_2$, 5 mM Mg-ATP, and 10 mM Hepes, pH 7.35. The bath solution consisted of: 140 mM NaCl or CsCl, 2.5 mM $BaCl_2$ or $CaCl_2$, 1 mM $MgCl_2$, 5 mM glucose, and 5 mM Hepes, pH 7.4. Signals were amplified with an Axopatch 200B amplifier and 333kHz A/D system (Axon Instruments, Union City, CA). Data were analyzed with CLAMPFIT 8 (Axon) and ORIGIN statistical software (OriginLab, Northampton, MA). There was no difference in the Rem inhibition of Ca^{2+} channel current expression for either Ca^{2+} or Ba^{2+} as the charge carrier. All recordings were performed at room temperature (20–22°C).

Cytosolic Calcium Imaging. Replication-deficient adenoviruses expressing GFP as a marker protein and Rem were constructed as described (10). C2C12(A) cells were infected with Ad-Ctr or Ad-Rem adenoviruses, placed in differentiation media (DM) for 6 days to induce robust Ca^{2+} channel expression (11–13), and then loaded with 1 μM fura 2 acetoxymethyl ester (fura 2-AM) with 1:1 dilution of Pluronic F127 (Molecular Probes) for 5 min at 37°C in a 5% CO_2 humidified incubator. Deesterification and removal of unincorporated fura 2-AM was accomplished by rinsing cells for 20–30 min in imaging bath solution containing 140 mM NaCl, 4 mM KCl, 1 mM $MgCl_2$, 1 mM $CaCl_2$, 1 mM $NaHPO_4$, 5 mM dextrose, and 10 mM Hepes, pH 7.4. All fura 2 imaging experiments were performed at 37°C. The coverslips

This paper was submitted directly (Track II) to the PNAS office.

Abbreviations: HA, hemagglutinin; RGK, Rem, Rem2, Rad, and Gem/Kir Ras-related GTP-binding proteins; DM, differentiation media.

‡To whom correspondence should be addressed. E-mail: dandres@uky.edu.

were mounted on a temperature-controlled chamber and placed on the stage of a Zeiss inverted epifluorescence microscope. The cells were excited with light of 340 and 380 nm wavelengths, and the emission wavelength, ≈510 nm, was collected and analyzed by using Axon Instruments IMAGING WORKBENCH. The images obtained at 340 and 380 nm were divided pixel by pixel, and the ratio data were reported. Background F340/380 was determined in Ca-free (EGTA) bath solutions with permeabilized cells.

C2C12 Ca^{2+} transients were elicited with a rapid (<3-s) bulk flow of equimolar replacement of NaCl with 40 mM KCl. The resulting transients were monitored at a sample frequency of 2–4 Hz. Before fura 2 imaging, GFP fluorescence (excitation 488 nm) was recorded at 510 nm. The GFP image for a given field was first saved, and then 340- and 380-nm fluorescence was measured. Cells infected with control virus exhibited variable luminosities of 488-nm signal but had indistinguishable Ca^{2+} transients from myotubes in the same field that displayed no 488-nm signal. Therefore, Rem effects were assessed by performing statistical tests on adenoviral infected cells in a given field by sorting cells into two groups: either visible GFP signal (488 nm) or no visible GFP signal. To measure total Ca^{2+} flux in response to a KCl-induced depolarization, transients were integrated over the first 50 s of 40 mM KCl exposure. Within a given field, separate integrals were averaged for either GFP-positive or -negative cells. A paired *t* test was performed to compare the total Ca^{2+} GFP-positive to nondetectable GFP signals. Fields were preselected to contain ≈50% infected myotubes.

Rem-Ca$_V\beta$ Subunit Interactions. Hemagglutinin (HA)-Rem pCDNA, HA-Rem$^{1–282}$, HA-Rem$^{1–265}$, or HA-Rad pCDNA and either Flag-Ca$_V\beta_{2a}$ pCMV-T7F2, Flag-Ca$_V\beta_{1b}$, Flag-Ca$_V\beta_{4a}$, or pCMV-T7F2 were cotransfected into HEK293 cells by the calcium phosphate method (8). Forty-eight hours posttransfection, the cells were washed with PBS, placed into 1 ml of Verseen (GIBCO), harvested, pelleted, and then suspended in ice-cold immunoprecipitation (IP) buffer [20 mM Tris, pH 7.5/250 mM NaCl/1% TX-100/0.5 mM DTT/1× protease inhibitor mixture (Calbiochem)/10 mM $MgCl_2$/10 μM GTPγS]. The cells were lysed, subjected to centrifugation, and 1 mg of the supernatant incubated in a 500-μl reaction containing 10 μl of packed Protein G Sepharose (Pharmacia) and 4 μg of anti-Flag M2 monoclonal antibody (Sigma) for 3 h with gentle rotation at 4°C. The beads were pelleted and 5 μl of the supernatant saved for analysis. The beads were then washed three times with 1 ml of IP buffer. The supernatant and bound fractions were resolved on SDS/PAGE, transferred to nitrocellulose, and subjected to immunoblot analysis. HA-Rem and HA-Rad were detected by immunoblotting as described (7), except that the biotinylated HA antibody was used at 1 μg/ml, and bound protein was detected with streptavidin–horseradish peroxidase (Pierce) at a 1:40,000 dilution. The blot was subsequently probed for Flag-Ca$_V\beta_{2a}$ by incubating the membranes with anti-Flag M2 monoclonal antibody (1 μg/ml) to confirm the efficiency of immunoprecipitation.

Results

Rem Expression During C2C12 Myoblast Differentiation. Rem mRNA is abundantly expressed in mouse cardiac and skeletal muscle (1). To identify a cellular system in which to examine the contribution of Rem to muscle function, RNase protection analysis was used to assess Rem expression (1). Total RNA was isolated from the myoblast cell lines C2C12, L6, and MM14, from primary mouse skeletal muscle and cardiac myocytes, and from 10T1/2 and 3T3 fibroblast cell lines, and used for RNase protection analysis. Rem mRNA was detected in each of the myoblast cell lines and in primary mouse skeletal and cardiac myocytes examined but not in fibroblast cell lines (Fig. 1*A*). To confirm that C2C12 cells expressed Rem protein, we performed

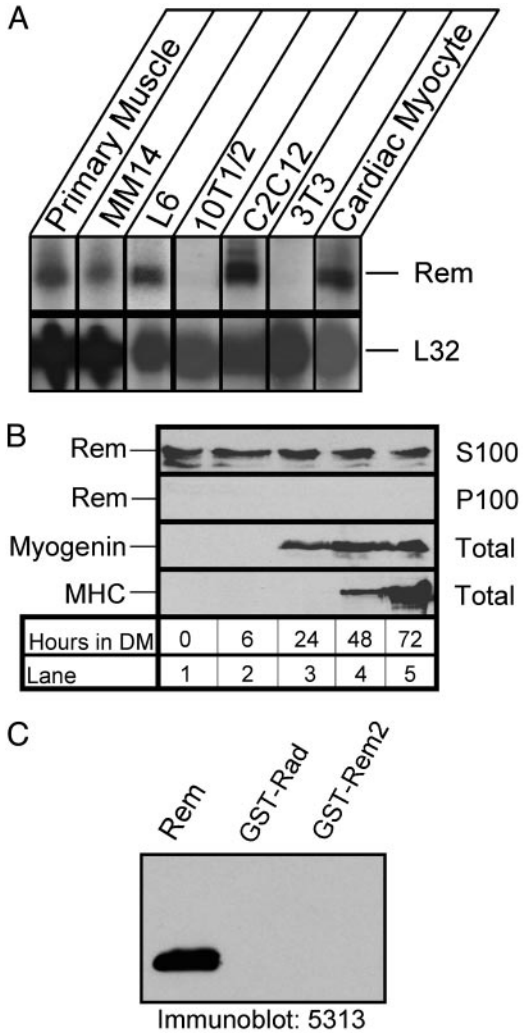

Fig. 1. Muscle expression of Rem. (*A*) Total RNA (20 μg) from the indicated primary muscle cell cultures and cell lines was hybridized with radiolabeled antisense Rem and L32 riboprobes and then subjected to RNase protection analysis. (*B*) C2C12DS myoblasts were cultured and differentiated into myotubes by replacing the growth media with DM; cell lysates were harvested at the indicated time, fractionated into a 100,000 × *g* soluble (S100) and particulate (P100) fractions, and subjected to immunoblot analysis. Rem expression was analyzed in both fractions with the 5313 antibody; myogenin expression was analyzed with the F5D monoclonal antibody, and myosin heavy chain (MHC) expression was analyzed with the MF-20 antibody, as indicated on the left. (*C*) Immunoblot analysis using affinity-purified anti-Rem (5313) antibody.

immunoblots with a polyclonal antipeptide antibody directed against amino acids 6–17 of Rem. Fig. 1*B* shows that this antibody reacted with a protein that migrated on SDS gels with an apparent molecular weight of 42,000 and bound strongly to recombinant Rem but did not bind detectably to other RGK family proteins (Fig. 1*C*). Antibody binding to this 42-kDa protein was abolished in the presence of the synthetic peptide used to make the antibody, and transfection of HEK293 cells with a recombinant Rem expression plasmid produced a 42-kDa protein by immunoblot analysis (data not shown).

C2C12 cells have been used extensively as an *in vitro* model of skeletal muscle differentiation (14). Under the conditions used in this study, myotubes began to form 2 days after transfer to DM, and the majority of cell nuclei were present in large multinucleate myotubes after 4 days in DM (see Fig. 6, which is published as supporting information on the PNAS web site).

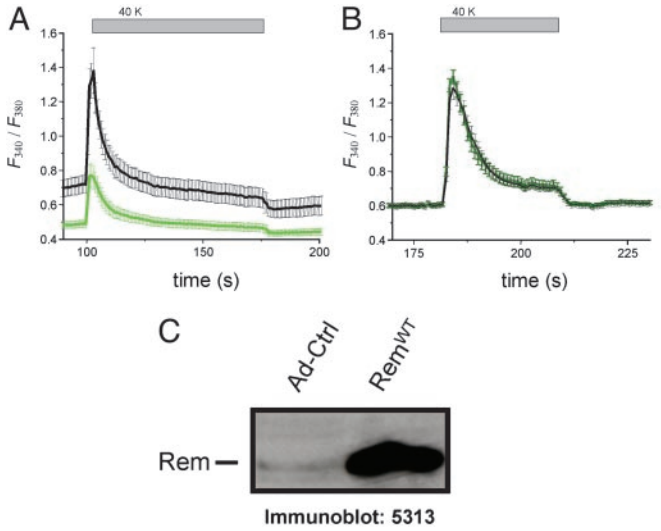

Fig. 2. Rem inhibits depolarization-induced Ca^{2+} transients in C2C12 myotubes. Representative Ca^{2+} transients recorded from multiple myotubes in a given field. (*A*) C2C12 myotubes infected with Rem-GFP. The Ca^{2+} transient was elicited by 40 mM K induced depolarization. The black line represents average response of cells that did not express GFP fluorescence; the green line is transient recorded from myotubes from the same field expressing the GFP signal. (Bars = SE.) (*B*) C2C12 myotubes infected with control adenovirus expressing unfused GFP. (*C*) Cell lysates from adenoviral infected C2C12 cells were incubated with anti-Rem antibody for immunoblot analysis.

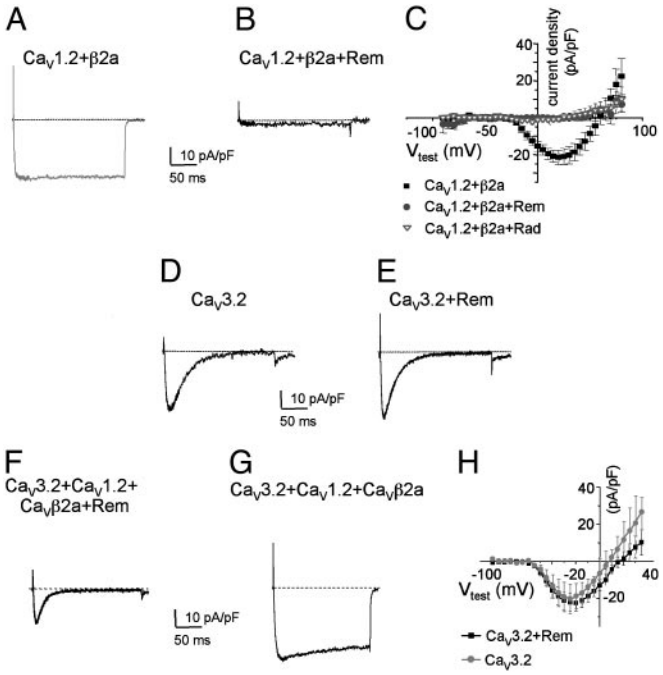

Fig. 3. Rem and Rad prevent *de novo* expression of $Ca_V1.2$ ionic current but not T type Ca^{2+} currents. (*A*) Representative Ba^{2+} current elicited by a voltage step from −80 to 10 mV in HEK293 cells transiently transfected with expression vectors encoding $Ca_V1.2$, β_{2a}, and GFP. (Bars = 10 pA/pF and 50 ms.) (*B*) HEK293 cells cotransfected with $Ca_V1.2$, β_{2a}, and GFP-tagged wild-type Rem or Rad (same conditions as *A*). No current is detectable. (*C*) Current–voltage relationships for cells transfected with $Ca_V1.2$, β_{2a}, and unfused GFP (filled squares) or $Ca_V1.2$, β_{2a}, and GFP-Rem (filled circles) or Rad (open triangles). Average and SE from six to eight experiments for each group are shown. (*D* and *E*) Representative control $Ca_V3.2$ ionic current and $Ca_V3.2$ ionic current coexpressed with GFP-Rem. Also, coexpression of β_{2a} with $Ca_V3.1$ or 3.2 or coexpression of $Ca_V\beta_{2a}$, GFP-Rem, and $Ca_V3.1$ or 3.2 had no effect on T type Ca^{2+} channel current expression (data not shown for $Ca_V3.1$). (*F* and *G*) Coexpression of $Ca_V3.2$, $Ca_V1.2$, β2a display a complex kinetic pattern that resolves to an ionic current that on Rem expression is indistinguishable from the $Ca_V3.2$ expressed alone. (*H*) The current–voltage curve shows that $Ca_V3.2$ current amplitude expression is not altered by Rem coexpression. Average and SE from six to eight experiments for each group are shown.

C2C12 cells expressed Rem protein regardless of cell density, and Rem expression remained constant throughout the differentiation process (Fig. 1*B*). To investigate the potential mechanistic importance of Rem function during myoblast differentiation, we generated replication-defective adenovirus engineered to express either wild-type Rem or a control virus containing the Rem cDNA cloned in the reverse orientation. These adenoviruses express the GFP gene under the control of a separate promoter, allowing the direct observation of the efficiency of infection by following GFP expression (10, 15). Rem overexpressing cells did not differ from control cells or uninfected cells in gross morphology or in their ability to differentiate into mature myotubes, suggesting that Rem does not control myogenic differentiation (Fig. 6).

Rem Inhibits L Type Ca^{2+} Channel Function in C2C12 Cells. Voltage-gated Ca^{2+} channels play essential roles in many cellular functions, including excitation–contraction coupling in muscle cells (16). Recent studies suggest that the Rem-related protein Gem regulates Ca^{2+} channel function (17). To determine whether Rem acts similarly, C2C12 cells were infected with Rem or control adenovirus and induced to differentiate by exposure to DM for 6 days (Fig. 2*C*). To assess the role of voltage-gated Ca^{2+} channels in triggering Ca^{2+} entry, we activated channels by KCl-induced depolarization. Addition of 40 mM KCl elicits a Ca^{2+} transient in all C2C12 myotubes tested (Fig. 2). However, myotubes overexpressing exogenous Rem had significantly reduced transients compared with uninfected myotubes (Fig. 2*A*; $P = 0.003$, $n = 39$ Rem-infected vs. 33 noninfected cells in five fields). The mean difference of the response between GFP-positive and nondetectable-GFP cells (five fields) after Rem adenovirus exposure was 14.2 ± 3.2, whereas control virus-infected C2C12 cells showed no significant difference in the Ca^{2+} transients to uninfected cells (mean difference was –1 ± 0.6) (Fig. 2*B*).

Rem Inhibits L Type, but Not T Type, Ca^{2+} Channel Function. Myoblasts express two classes of voltage-gated Ca^{2+} channel: in the early stages of differentiation, T type ($Ca_V3.2$) channels are essential for fusion (18), and during differentiation, L type channel expression becomes prominent (12, 19). The experiments of Fig. 2 suggested that Rem expression resulted in the attenuation of L type Ca^{2+} current, because slow depolarization would be expected to voltage inactivate T type channels (20). Therefore, we next tested the ability of Rem to prevent current expression of heterologously expressed L type (Ca_V1) or T type (Ca_V3) Ca^{2+} channels.

As seen in Fig. 3*A*, HEK293 cells transiently cotransfected with $Ca_V1.2$ and $Ca_V\beta_{2a}$ express >20 pA/pF of peak inward current. In contrast, coexpression of wild-type Rem with $Ca_V1.2$ and $Ca_V\beta_{2a}$ results in a complete absence of detectable ionic current expression (Fig. 3*B*). $I_{Ca,L}$ was undetectable for all potentials when coexpressed with Rem (Fig. 3*C*). These results are consistent with the ability of the Gem GTPase to prevent L type Ca^{2+} current expression (17). Next, we tested the effect of Rem coexpression on $Ca_V3.2$ function, the T type channel expressed by skeletal myoblasts. To control for any nonspecific effects of Rem on current expression, we coexpressed Rem with the T type Ca^{2+} channels, $Ca_V3.1$ or $Ca_V3.2$, with or without the auxiliary $Ca_V\beta$ subunit, even though $Ca_V3.2$ channels do not require accessory subunits for ionic current expression (21, 22). $Ca_V\beta$ subunit coexpression had no effect on Ca_V3 channel

PHYSIOLOGY

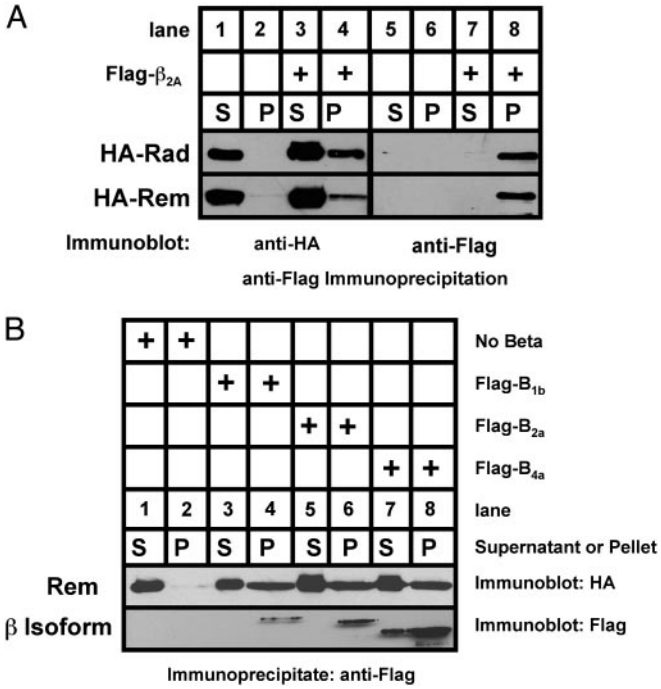

Fig. 4. *In vivo* interaction of Rem and Rad with $Ca_V\beta_{2a}$. (*A*) HEK293 cells were cotransfected with expression vectors encoding HA-tagged Rem or Rad with or without a vector encoding Flag-tagged $Ca_V\beta 2a$. Cell extracts were prepared, 1 mg of the supernatant was subjected to immunoprecipitation with anti-FLAG antibody in a 500-μl reaction volume, and the entire bound fraction or 5 μl of the unbound fraction was analyzed by immunoblotting with anti-HA to detect Rem/Rad (left) and anti-Flag to detect $\beta 2a$ (right). (*B*) Coimmunoprecipitation analysis demonstrates association of Rem and both $\beta 1b$ and $\beta 4a$.

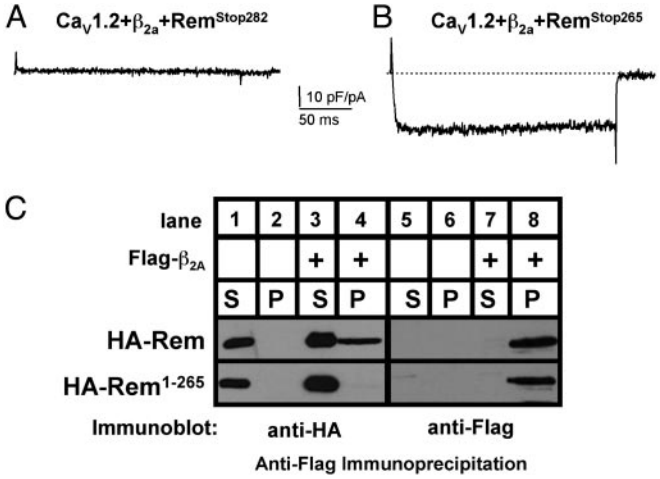

Fig. 5. Effects of Rem C-terminal mutants on Ca^{2+} channel current expression. Representative Ba^{2+} current elicited by a voltage step from −80 to 10 mV in HEK293 cells transiently transfected with expression vectors encoding $Ca_V1.2$, β_{2a}, and either GFP-$Rem^{Stop282}$ (*A*) or GFP-$Rem^{Stop265}$ (*B*). (Bars = 10 pA/pF and 50 ms.) (*C*) HEK293 cells transiently cotransfected with expression vectors encoding HA-tagged Rem or HA-$Rem^{Stop265}$ and either Flag-$Ca_V\beta_{2a}$ or empty Flag vector. Whole-cell extracts were immunoprecipitated with anti-FLAG antisera and analyzed by immunoblotting as described in Fig. 4. Data are representative of a typical experiment performed three independent times.

current expression (data not shown). In contrast to L type ionic current expression, Rem did not inhibit expression of currents through the Ca_V3 family of channels [average peak current densities for $Ca_V3.2$ alone, -22.2 ± 4.4 pA/pF ($n = 8$); $Ca_V3.2$ and Rem, -20.1 ± 8.0 ($n = 8$)] (Fig. 3 *D* and *E*; similar results were seen for $Ca_V3.1$). Furthermore, Rem had no effect on Ca_V3 functional properties (Fig. 3*E*). Finally, we tested the ability of Rem to selectively regulate L type Ca^{2+} currents in cells coexpressing $Ca_V1.2$, $Ca_V\beta_{2a}$, and $Ca_V3.2$. As expected, coexpression of functional $Ca_V1.2$ and $Ca_V3.2$ channels showed a complex kinetic pattern (Fig. 3*G*), but expression of Rem in these cells resulted in ionic current similar to $Ca_V3.2$ alone (Fig. 3 *D* and *F*).

Because Rad is also expressed in muscle, the effects of wild-type Rad on heterologously expressed L type Ca^{2+} channels was examined. Coexpression of Rad with $Ca_V1.2$ and $Ca_V\beta_{2a}$ results in a complete inhibition of detectable ionic current expression (Fig. 3*C*). Taken together, these data strongly support the notion that both Rem and Rad serve as regulators of L type Ca^{2+} channel activity.

Rem and Rad Bind to $Ca_V\beta$ Subunits. Gem has been reported to associate with $Ca_V\beta$ subunits (17). To determine whether Rem and Rad interact with Ca^{2+} channel β-subunits *in vivo*, HEK293 cells were transiently transfected with expression vectors encoding Flag-tagged $Ca_V\beta_{2a}$ alone or cotransfected with vectors expressing HA-tagged Rem or Rad. Flag-tagged $Ca_V\beta_{2a}$ was then isolated by immunoprecipitation and bound HA-tagged proteins visualized by SDS gel electrophoresis and immunoblotting. As seen in Fig. 4*A* (compare lanes 2 and 4), HA-tagged Rem and Rad were found in the pelleted fraction in a Flag-$Ca_V\beta_{2a}$-dependent manner. HA-tagged Rem was also found to interact with $Ca_V\beta 1b$ and $Ca_V\beta 4a$, indicating that Rem can directly interact with a variety of β-subunit isoforms (Fig. 4*B* top, lanes 4 and 8). Thus, both Rem and Rad proteins demonstrate direct interaction with $Ca_V\beta$ subunits.

Rem C-Terminal Domain Is Crucial for Regulation of Ca^{2+} Channel Function. Although Rem, Rad, and Gem each directly associates with β subunits, they have distinct effector domains, which is significant because the effector domain of Ras-related GTPases plays a central role in defining cellular effector protein interactions and is often perfectly conserved within Ras subfamilies (1, 2). However, RGK GTPases all contain an extended and highly conserved polybasic C-terminal domain, suggesting a possible role for this domain in their function (2, 7). To determine the importance of the C terminus to Rem-mediated regulation of Ca^{2+} channel function, a series of Rem C-terminal deletion mutants were generated and examined for their ability to regulate Ca^{2+} channel activity. As seen in Fig. 5, coexpression of $Ca_V1.2$, β_{2a}, and a short C-terminal deletion ($Rem^{Stop282}$) resulted in a complete absence of Ca^{2+} channel function, whereas coexpression of a larger deletion ($Rem^{Stop265}$) resulted in expression of current densities that were the same as expressing the empty GFP control vector [mean current density $Rem^{Stop282}$: 0 current ($n = 8$); $Rem^{Stop265}$: -26.2 ± 11.1 pA/pF ($n = 5$)]. Identical results were seen when $Rad^{Stop276}$, containing an equivalent C-terminal deletion to the conserved C-terminal domain of Rad, was coexpressed with $Ca_V1.2$ and $Ca_V\beta_{2a}$ (data not shown). Thus, the C-terminal 32 amino acids in Rem and Rad contain residues that play a critical role in Rem- and Rad-mediated inhibition of Ca^{2+} channel function.

We next asked whether the Rem C-terminal domain was necessary for β-subunit interaction. Although Flag-tagged $Ca_V\beta_{2a}$ interacted with wild-type Rem, the deletion of residues 265–282 within the C-terminal domain greatly reduced $Ca_V\beta_{2a}$ binding (Fig. 5*C*, compare lanes 4 and 8). These results suggest that the C-terminal domain is necessary for Rem-mediated regulation of L type Ca^{2+} channel activity, in part by contributing to $Ca_V\beta_{2a}$ binding.

Discussion

The most important finding in this study is that two members of the RGK GTPase family, Rem and Rad, have a common cellular function. Both GTPases block L type Ca^{2+} channel current expression via interactions with auxiliary $Ca_V\beta$ subunits. Coupled with recent findings for a third member of this family, Kir/Gem (17), we now propose that regulation of Ca^{2+} channel expression via $Ca_V\beta$ interaction is a general function of all RGK GTPases. Moreover, the regulation of Ca^{2+} channel density is central to the regulation of skeletal muscle function. Because Rem and Rad are both expressed in skeletal muscle myotubes, we suggest that these GTPases represent a previously unrecognized regulatory mechanism for regulating muscle cell Ca^{2+} signaling.

Although Rem and Rad operate via a common mechanism, their expression is temporally distinct. Striated muscle cells, including skeletal muscle myoblasts, myotubes and cardiac myocytes express Rem, and Rem expression is unchanged during myogenic differentiation (Fig. 1). This profile contrasts with Rad, which is not expressed in proliferating myoblasts (23) or Gem, which is not expressed in muscle cells (3, 4). To directly examine the involvement of Rem in myoblast differentiation, we infected C2C12 cells with recombinant adenovirus and assessed the effects of wild-type Rem expression on C2C12 differentiation. C2C12 cells overexpressing Rem undergo differentiation and continue to express muscle-specific marker proteins that are a hallmark of normal adult muscle (see Fig. 6), demonstrating that the process of myogenic differentiation is not overtly affected by Rem expression.

Using a calcium-sensitive dye and fluorescence microscopy to monitor changes in the cytosolic free Ca^{2+} concentration in differentiated C2C12 cells, we demonstrate that Rem-expressing C2C12 myotubes have significantly reduced Ca^{2+} transients compared with uninfected myotubes or GFP-expressing control virus-infected cells (Fig. 2). Taken together with Rem blockade of Ca^{2+} current expression, these data indicate that Rem regulates myoblast Ca^{2+} channel function, which raises an interesting point. As with mature skeletal muscle, the differentiated C2C12 intracellular store Ca^{2+} release can be triggered by depolarization via electrical stimulation but without appreciable trans-plasma-membrane Ca^{2+} influx (e.g., ref. 23). In that same study, 40 mM KCl induced transients that were inhibited by 10 μM nifedipine, but only after a 30-min incubation. This result is consistent with the contribution of long-term Ca^{2+} entry via L type Ca^{2+} channels. Also, recent reports of fusing myoblasts showed that window current via T, and presumably L, type channels may contribute to cytosolic Ca^{2+} (18). In other words, voltage-gated Ca^{2+} channels permit a steady-state influx of Ca^{2+} to the cytosol. More to the point of the present study, our data concur that the L type channels' contribution may be setting tonic Ca^{2+} levels in the cytosol.

Recent studies suggest that RGK proteins regulate cytoskeleton dynamics (24–26). Because reorganization of the cytoskeleton might interfere with Ca^{2+} channel function, it is important to distinguish between selective Rem-dependent effects on Ca^{2+} channels and a general blockade of protein sorting. The absence of any obvious effects on the actin cytoskeleton after adenovirus-mediated expression of wild-type Rem in C2C12 myoblasts, as monitored by immunostaining with Texas red phalloidin (data not shown), or on T type Ca^{2+} channel current expression (Fig. 3*E*), which are synthesized in the endoplasmic reticulum and must undergo proper intracellular trafficking to be functionally expressed at the plasma membrane, is consistent in both cases with the specific inhibition of Ca_V1 function by Rem.

The intracellular trafficking of Ca^{2+} channels from their site of synthesis in the endoplasmic reticulum to the cell surface is an absolute requirement for their function (16). Ca^{2+} channel α_1 subunits contain cytoplasmic endoplasmic reticulum retention signals, which act to prevent the expression of ion channels at the cell surface (27). Coexpression of auxiliary cytoplasmic $Ca_V\beta$ subunits masks these retention signals and allows for expression of functional channels in the plasma membrane (28). Recent studies have suggested that binding of the Gem GTPase to β-subunits inhibits their assembly with Ca^{2+} channel α_1 subunits, such that coexpressing Gem eliminated Ca^{2+} channel expression (17). In this regard, the predominant localization of Rem to the cytoplasm (Fig. 1*B* and ref. 2) may act to sequester Rem:$Ca_V\beta$–subunit complexes from the membrane fraction and inhibit Ca^{2+} channel expression at the cell surface. However, coimmunoprecipitation studies suggest that only a fraction of total Rem and Rad protein is found in association with $Ca_V\beta$ subunits when overexpressed in HEK293 cells (Fig. 4), although it is possible that muscle-specific proteins may stabilize the complex or that yet- to-be-defined posttranslational modification(s) or GTP binding may stabilize a higher-affinity complex. In parallel, $Ca_V\beta$ regulation of $Ca_V\alpha$ is a dynamic process that may involve transient association of preformed channels in the surface membrane (29). This information, coupled with our finding that Rem and Rad potently inhibit L type but not heterologously expressed T type Ca^{2+} channels (Fig. 3 *C*, *E–G*), suggests that regulation occurs in $Ca_V\beta$-dependent fashion but may not involve a blockade of functional L type Ca^{2+} channel trafficking. Our results also indicate an important role for the Rem and Rad C terminus in $Ca_V\beta$-subunit binding (Fig. 5). The C-terminal domains of Rad and Gem contain calmodulin-binding regions, whereas Rem and Rad interact with 14–3-3 proteins in a phosphorylation-dependent manner within this domain, suggesting a possible link between these GTPases and both calcium and kinase signaling events (7, 30, 31).

The potential importance of RGK-mediated regulation of voltage-dependent Ca^{2+} channels is highlighted by recent genetic study by Lynch *et al*. (32), which has defined a link between a nonsynonymous single-nucleotide polymorphism within the Rad gene (Rad^{Q66P}) and patients with congestive heart failure. The finding that Rad efficaciously inhibits *de novo* expression of L type Ca^{2+} channels (Fig. 3*C*) suggests that the Rad^{Q66P} mutation may be causative for disease by virtue of its regulation of Ca^{2+} entry. Clearly, additional studies will be needed to clarify the upstream signals that regulate Rem/Rad activity and the structural basis of $Ca_V\beta$-subunit association, the effects of Rem/Rad expression on the interaction of α_1:β-subunits, and the subcellular localization of both $Ca_V\beta$ and α_1 subunits on RGK protein expression.

Conclusion

The expression of Rem and Rad in skeletal and cardiac muscle, together with their dynamic effects on Ca^{2+} channel function, suggests that they play important roles in the regulation of intracellular Ca^{2+} signaling. In particular, we demonstrate that Rem and Rad regulate the activity of voltage-dependent Ca^{2+} channels in a $Ca_V\beta$-subunit-dependent fashion. Our present results indicate that the RGK GTPase family may provide a mechanism for achieving cross talk between Ras-related GTPases and electrical signaling pathways. Further investigations are necessary to understand the role of Rem and Rad in regulating voltage-dependent Ca^{2+} channels and how RGK-mediated changes in the individual response properties of voltage-sensitive ion channels may effect excitation–contraction coupling and calcium-signaling pathways in cardiac and skeletal muscle.

The excellent technical assistance of Renee Bartlett is gratefully acknowledged. We also thank Drs. P. Bonner and R. Krauss for muscle cell lines; Dr. T. Kamp (University of Wisconsin, Madison) for the $Ca_V1.2$ and $Ca_V\beta2a$ plasmids; and members of the laboratory for comments on the manuscript. This work was supported in part by the American Heart Association [(to D.A.A.); J.S. is an Established Investigator of the American Heart Association]; and by National Institutes of Health Grants HL072936 (to D.A.A.), HL63416, and HL74091 (to J.S.).

1. Finlin, B. S. & Andres, D. A. (1997) *J. Biol. Chem.* **272,** 21982–21988.
2. Finlin, B. S., Shao, H., Kadono-Okuda, K., Guo, N. & Andres, D. A. (2000) *Biochem. J.* **347,** 223–231.
3. Cohen, L., Mohr, R., Chen, Y. Y., Huang, M., Kato, R., Dorin, D., Tamanoi, F., Goga, A., Afar, D., Rosenberg, N., *et al*. (1994) *Proc. Natl. Acad. Sci. USA* **91,** 12448–12452.
4. Maguire, J., Santoro, T., Jensen, P., Siebenlist, U., Yewdell, J. & Kelly, K. (1994) *Science* **265,** 241–244.
5. Reynet, C. & Kahn, C. R. (1993) *Science* **262,** 1441–1444.
6. Kang, J. S., Mulieri, P. J., Miller, C., Sassoon, D. A. & Krauss, R. S. (1998) *J. Cell Biol.* **143,** 403–413.
7. Finlin, B. S. & Andres, D. A. (1999) *Arch. Biochem. Biophys.* **368,** 401–412.
8. Andres, D. A., Shao, H., Crick, D. C. & Finlin, B. S. (1997) *Arch. Biochem. Biophys.* **346,** 113–124.
9. Zhang, Y., Cribbs, L. L. & Satin, J. (2000) *Am. J. Physiol.* **278,** H184–H193.
10. He, T. C., Zhou, S., da Costa, L. T., Yu, J., Kinzler, K. W. & Vogelstein, B. (1998) *Proc. Natl. Acad. Sci. USA* **95,** 2509–2514.
11. McMahon, D. K., Anderson, P. A., Nassar, R., Bunting, J. B., Saba, Z., Oakeley, A. E. & Malouf, N. N. (1994) *Am. J. Physiol.* **266,** C1795–C1802.
12. Lorenzon, P., Giovannelli, A., Ragozzino, D., Eusebi, F. & Ruzzier, F. (1997) *Eur. J. Neurosci.* **9,** 800–808.
13. Varadi, G., Orlowski, J. & Schwartz, A. (1989) *FEBS Lett.* **250,** 515–518.
14. Blau, H. M., Chiu, C. P. & Webster, C. (1983) *Cell* **32,** 1171–1180.
15. Spencer, M. L., Shao, H., Tucker, H. M. & Andres, D. A. (2002) *J. Biol. Chem.* **277,** 17605–17615.
16. Catterall, W. A. (2000) *Annu. Rev. Cell Dev. Biol.* **16,** 521–555.
17. Beguin, P., Nagashima, K., Gonoi, T., Shibasaki, T., Takahashi, K., Kashima, Y., Ozaki, N., Geering, K., Iwanaga, T. & Seino, S. (2001) *Nature* **411,** 701–706.
18. Bijlenga, P., Liu, J. H., Espinos, E., Haenggeli, C. A., Fischer-Lougheed, J., Bader, C. R. & Bernheim, L. (2000) *Proc. Natl. Acad. Sci. USA* **97,** 7627–7632.
19. Schmid, A., Renaud, J. F., Fosset, M., Meaux, J. P. & Lazdunski, M. (1984) *J. Biol. Chem.* **259,** 11366–11372.
20. Satin, J. & Cribbs, L. L. (2000) *Circ. Res.* **86,** 636–642.
21. Lacinova, L., Klugbauer, N. & Hofmann, F. (1999) *J. Physiol.* **516,** 639–645.
22. Cribbs, L. L., Lee, J. H., Yang, J., Satin, J., Zhang, Y., Daud, A., Barclay, J., Williamson, M. P., Fox, M., Rees, M. & Perez-Reyes, E. (1998) *Circ. Res.* **83,** 103–109.
23. Huang, C. F., Flucher, B. E., Schmidt, M. M., Stroud, S. K. & Schmidt, J. (1994) *Neuron* **13,** 167–177.
24. Ward, Y., Yap, S. F., Ravichandran, V., Matsumura, F., Ito, M., Spinelli, B. & Kelly, K. (2002) *J. Cell Biol.* **157,** 291–302.
25. Piddini, E., Schmid, J. A., de Martin, R. & Dotti, C. G. (2001) *EMBO J.* **20,** 4076–4087.
26. Pan, J. Y., Fieles, W. E., White, A. M., Egerton, M. M. & Silberstein, D. S. (2000) *J. Cell Biol.* **149,** 1107–1116.
27. Walker, D. & De Waard, M. (1998) *Trends Neurosci.* **21,** 148–154.
28. Bichet, D., Cornet, V., Geib, S., Carlier, E., Volsen, S., Hoshi, T., Mori, Y. & De Waard, M. (2000) *Neuron* **25,** 177–190.
29. Garcia, R., Carrillo, E., Rebolledo, S., Garcia, M. C. & Sanchez, J. A. (2002) *J. Physiol.* **545,** 407–419.
30. Fischer, R., Wei, Y., Anagli, J. & Berchtold, M. W. (1996) *J. Biol. Chem.* **271,** 25067–25070.
31. Moyers, J. S., Bilan, P. J., Zhu, J. & Kahn, C. R. (1997) *J. Biol. Chem.* **272,** 11832–11839.
32. Lynch, R. A., Wagoner, L., Li, S., Sparks, L., Molkentin, J. & Dorn, G. W. II (2002) *Physiol. Genomics* **10,** 159–168.